Tailoring the magnetization reversal of elliptical dots using exchange bias (invited)

J. Sort, K. S. Buchanan, J. E. Pearson, A. Hoffmann, E. Menéndez, G. Salazar-Alvarez, M. D. Baró, M. Miron, B. Rodmacq, B. Dieny, and J. Nogués

Citation: Journal of Applied Physics **103**, 07C109 (2008); doi: 10.1063/1.2840467
View online: http://dx.doi.org/10.1063/1.2840467
View Table of Contents: http://scitation.aip.org/content/aip/journal/jap/103/7?ver=pdfcov
Published by the AIP Publishing

Tailoring the magnetization reversal of elliptical dots using exchange bias (invited)

J. Sort,[1,a)] K. S. Buchanan,[2] J. E. Pearson,[3] A. Hoffmann,[2,3] E. Menéndez,[4] G. Salazar-Alvarez,[5] M. D. Baró,[4] M. Miron,[6] B. Rodmacq,[6] B. Dieny,[6] and J. Nogués[7]
[1]*Institució Catalana de Recerca i Estudis Avançats (ICREA) and Departament de Física, Universitat Autònoma de Barcelona, 08193 Bellaterra, Barcelona, Spain*
[2]*Center for Nanoscale Materials, Argonne National Laboratory, Argonne, Illinois 60439, USA*
[3]*Materials Science Division, Argonne National Laboratory, Argonne, Illinois 60439, USA*
[4]*Departament de Física, Universitat Autónoma de Barcelona, 08193 Bellaterra, Spain*
[5]*Institut Català de Nanotecnologia, Edifici CM7, Campus Universitat Autónoma de Barcelona, 08193 Bellaterra, Spain*
[6]*SPINTEC (URA 2512 CNRS/CEA), CEA/Grenoble, 17 Av. Martyrs, 38054 Grenoble Cedex 9, France*
[7]*Institució Catalana de Recerca i Estudis Avançats (ICREA) and Institut Català de Nanotecnologia, Edifici CM7, Campus Universitat Autónoma de Barcelona, 08193 Bellaterra, Spain*

(Presented on 8 November 2007; received 6 September 2007; accepted 16 January 2008; published online 5 March 2008)

Exchange bias effects have been studied in elliptical dots composed of ferromagnetic $Ni_{80}Fe_{20}$–antiferromagnetic $Ir_{20}Mn_{80}$ bilayers. The magnetization reversal mechanisms and magnetic configurations have been investigated by magneto-optic Kerr effect and magnetic force microscopy. Although the obtained bias fields in these dots are relatively small, the magnetization reversal is found to be influenced by the ferromagnetic–antiferromagnetic coupling. Namely, for some off-axis angles of measurement, the magnetization reversal mechanism of the $Ni_{80}Fe_{20}-Ir_{20}Mn_{80}$ ellipses depends on whether exchange bias is induced along the minor or major axis of the ellipses. Hence, exchange bias is shown to be an effective means for tailoring the magnetization reversal of elliptical dots after sample fabrication. © *2008 American Institute of Physics*. [DOI: 10.1063/1.2840467]

INTRODUCTION

The coupling between ferromagnetic (FM) and antiferromagnetic (AFM) materials, also termed exchange bias, manifests itself by the occurrence of a shift of the hysteresis loop along the magnetic field axis and an enhancement of coercivity.[1,2] The first effect is typically ascribed to the pinning exerted by the interfacial AFM spins to the FM, while the coercivity enhancement is often attributed to irreversible dragging of AFM spins during reversal of the FM.[3] Both of these effects have led to important technological applications. The hysteresis loop shift is currently exploited in magnetic read heads and magnetic random access memories based on spin valves or tunneling junction structures.[4] The coercivity enhancement (and the associated increase of magnetic anisotropy) can be used to increase the magnetic hardness of permanent magnets[5] or to push the superparamagnetic limit of FM nanoparticles.[6]

In recent years, the tendency toward miniaturization of magnetic devices has triggered the study of exchange bias properties in lithographed FM-AFM nanostructures.[2,7,8] In particular, the competition between magnetostatic energy and exchange bias in circular dots can result in novel phenomena, such as the change of magnetization reversal mechanism as a function of the angle of measurement[8] or the occurrence of the so-called displaced vortex states.[9] Although exchange bias has been investigated to some extent both in circular dots and rings,[8–11] reports on exchange bias effects in magnetic ellipses are scarce.[12] Note that the magnetization reversal mechanism (i.e., rotation versus vortex formation) in exchange biased circular dots has been so far controlled by structural parameters (e.g., dot size) and interface coupling effects (e.g., magnitude of the loop shift).[9] However, due to their symmetry, other effects, such as the direction of the cooling field, play no role in the magnetization reversal mechanism. Indeed, in circular dots, the relative orientation of the applied field to the exchange bias field is the only relevant parameter giving rise to a critical angle, where the magnetization reversal changes from coherent rotation to vortex nucleation and annihilation.[8,9] However, in elliptical structures the situation is more complex, since the elliptical shape introduces additional shape anisotropy, whose direction with respect to the applied field and exchange bias is also important.

Therefore, in this article, we investigate the exchange bias properties of elliptical dots, with variable aspect ratio (and hence different degrees of shape anisotropy), composed of exchange coupled $Ni_{80}Fe_{20}-Ir_{20}Mn_{80}$ bilayers. It is observed that the nature of the magnetization reversal is mostly determined by the shape anisotropy and the exchange bias plays a lesser role compared to the circular dots. However, for certain combinations of aspect ratios and applied fields, varying the direction of the exchange bias can trigger a change of the magnetization reversal from a reversal via vortex formation to a reversal dominated by magnetization rotation.

a)Electronic mail: jordi.sort@uab.es.

EXPERIMENTAL DETAILS

A continuous film with the composition $Ta(5\ nm)/Ni_{80}Fe_{20}(30\ nm)/Ir_{20}Mn_{80}(5\ nm)/Pt(2\ nm)$ (where $Ni_{80}Fe_{20}$ is FM and $Ir_{20}Mn_{80}$ is AFM) was deposited onto a thermally oxidized Si wafer by dc magnetron sputtering. From the continuous film, arrays of elliptical disks with a minor axis of $2b=0.5\ \mu m$ and aspect ratios (ratio between the major and minor axes, a/b) of 1.5, 2, and 3 were fabricated by e-beam lithography and subsequent ion etching. The periodicity of the dots was 5 μm for the smaller dots and 7 μm for the larger, chosen to be $>2a$ to minimize interdot dipolar interactions. These patterned structures were heated to 480 K, which is above the blocking temperature of the system (estimated to be around 470 K) and, subsequently, field cooled (FC) in a $H_{FC}=3$ kOe magnetic field, applied either along the minor or the major axis of the ellipses. Hysteresis loops were measured at room temperature with fields applied at various in-plane angles from the FC direction, using a Durham Magneto Optics Kerr effect setup. Each presented loop corresponds to an average of 300 measured hysteresis loops. Since exchange bias systems typically exhibit variations in the exchange bias field and/or coercivity during the first few hysteresis cycles (i.e., the so-called training effect),[13] the data acquisition was started after having reversed ten times the magnetization of the patterned dots. In this way, the first few hysteresis loops are not part of the acquired data and the presented results correspond to the trained state, i.e., when no further variations of exchange bias or coercivity occur. The loops were corrected for the diamagnetic signal from the substrate. However, note that since this means subtracting a linear slope to the hysteresis loops, the overall shape of the loops (i.e., constricted versus nonconstricted) is not affected. Magnetic configurations were imaged at various magnetic fields using a Nanoscope III Digital Instruments, Inc., magnetic force microscope (MFM). Finally, a Landau–Lifshitz–Gilbert micromagnetic solver[14] was used to simulate the spin configurations of the system at some given magnetic field values after having induced the exchange bias either along the major or minor axis of the ellipses. Typical material parameters for bulk Permalloy were used: saturation magnetization $M_S=8\times10^{-5}$ A/m and exchange stiffness constant $A=1.3\times10^{-11}$ J/m. The exchange bias field was represented by an additional external field of 20 Oe, applied either along the major or minor axis of the ellipses. The magnetic configurations of the ellipses were obtained using cells of approximately $5\times5\ nm^2$. The simulations were started from an approximation of the desired final state and the system was allowed to relax toward equilibrium in fields matching those in the experiment. The MFM images were simulated from the calculated stray fields generated at a lift height of 100 nm.

RESULTS AND DISCUSSION

Shown in Fig. 1 are the hysteresis loops of the $Ni_{80}Fe_{20}/Ir_{20}Mn_{80}$ ellipses, with axis lengths equal to 0.5×0.75, 0.5×1, and $0.5\times1.5\ \mu m^2$, FC and measured along their minor [(a)–(c)] and major [(d)–(f)] axes. Constricted loops are observed along the minor axis of the ellipses, evidencing reversal via formation of a vortex state. This is in agreement with the previous reports on unbiased $Ni_{80}Fe_{20}$ ellipses.[15] The constriction is the least prominent for the most elongated ellipses. Moreover, a constriction in the central part of the loop is also observed for the $0.5\times0.75\ \mu m^2$ $Ni_{80}Fe_{20}-Ir_{20}Mn_{80}$ ellipses measured along their major axis. For larger aspect ratios, the loops recorded along the major axis tend to lose their central constriction and progressively become squarer, evidencing the increasing role of shape anisotropy, which tends to suppress reversal via single vortex state formation.

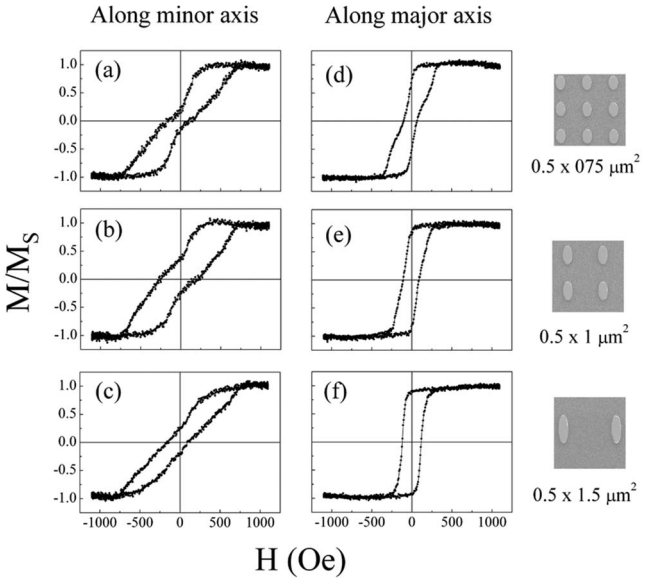

FIG. 1. [(a)–(c)] Hysteresis loops of $Ni_{80}Fe_{20}/Ir_{20}Mn_{80}$ ellipses, with dimensions of 0.5×0.75, 0.5×1, and $0.5\times1.5\ \mu m^2$, field cooled (FC) and measured along their minor axis. [(d)–(f)] Hysteresis loops of the same ellipses FC and measured along their major axis. Also shown are scanning electron microscopy images of the ellipses ($5\times5\ \mu m^2$ frames) with different aspect ratios.

The hysteresis loop shifts H_E are small, between 20 and 25 Oe for all the arrays. This is due to the relatively large $Ni_{80}Fe_{20}$ thickness. H_E of the corresponding continuous $Ni_{80}Fe_{20}/Ir_{20}Mn_{80}$ bilayer was found to be around 20 Oe. It is noteworthy that the vortex nucleation and annihilation fields, evaluated from the loops recorded along the minor axis, tend to increase with the aspect ratio, as it has been reported in the literature for pure $Ni_{80}Fe_{20}$.[16] This indicates that the stability of the vortex state is enhanced along this direction for larger aspect ratios.

MFM imaging has been used, together with the magneto-optic Kerr effect (MOKE) measurements, to shed light onto the magnetization reversal mechanisms when H_E is along the major axis of the ellipses. The images reveal that, as a general trend, when the ellipses are FC along the major axis, exchange bias tends to favor single domain states at remanence, in agreement with other results obtained on exchange biased patterned structures.[2,12,17] When this occurs, a strong dipolar contrast due to the stray fields emanated from the dots is obtained by MFM. This is clearly observable in panel (b), which corresponds to the $0.5\times1.5\ \mu m^2$ $Ni_{80}Fe_{20}/Ir_{20}Mn_{80}$ ellipses. For lower aspect ratios ($0.5\times0.75\ \mu m^2$ $Ni_{80}Fe_{20}/Ir_{20}Mn_{80}$ ellipses), a mixture of vortex

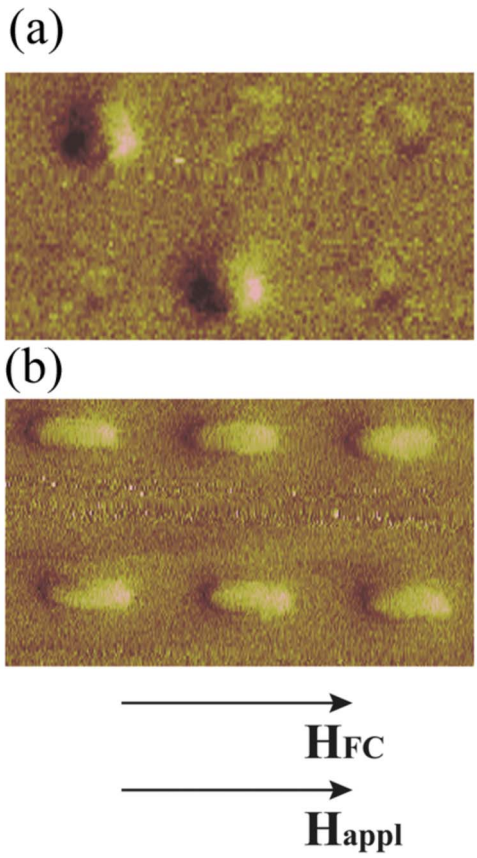

FIG. 2. (Color online) Magnetic force microscopy images recorded at remanence, after field cooling and saturating the ellipses along their major axis, corresponding to (a) the 0.5×0.75 μm^2 $Ni_{80}Fe_{20}/Ir_{20}Mn_{80}$ ellipses and (b) the 0.5×1.5 μm^2 $Ni_{80}Fe_{20}/Ir_{20}Mn_{80}$ ellipses.

and single domain states is observed at remanence [Fig. 2(a)]. Note that when the magnetization inside the ellipses forms vortex states, no magnetic fields are emanated from the dots and, consequently, virtually no magnetic contrast is observed by MFM. The mixture of single domain and vortex states observed in the ellipses with lower aspect ratio is the reason for the slightly constricted loop shape shown in Fig. 1(d). In the ellipses with higher aspect ratios, where MFM images reveal only single domain states [Fig. 2(b)], the hysteresis loops correspondingly lose the constriction in their central part [Figs. 1(e) and 1(f)].

It is noteworthy that for the range of geometries investigated the $Ni_{80}Fe_{20}/Ir_{20}Mn_{80}$ ellipses always reverse via vortex state formation (i.e., displaying a constricted hysteresis loop) when measured along their minor axis, independently of the direction along which exchange bias is induced. However, in some ellipses (particularly those with higher aspect ratio), the magnetization reversal at certain angles of measurement has been found to depend on the direction along which exchange bias has been previously established. This is illustrated in Fig. 3, where, although the direction of measurement is the same in both panels (a) and (b), the direction of the exchange bias (previously established by the field cooling procedure, as described in the experimental section) is different. As indicated in the bottom panels of Fig. 3, in (a) the exchange bias is induced by field cooling along the minor axis of the ellipses while in (b) the exchange bias is induced along their major axis. Note that although the direction of measurement is the same in (a) and (b), both the hysteresis loops recorded by MOKE and the MFM images are distinctly different depending on the thermomagnetic history of the sample. This occurs for angles of the field cooling direction ranging between 15° and 30° from the minor axis. For these angles, a clear vortex reversal is observed when the dots are FC along the major axis, while no clear vortex (no constriction) is observed if the dots are FC along the minor axis. Indeed, MFM imaging shows that in the latter case no vortex states nucleate before remanence [see the strong dipolar contrast in panel (a.1) in Fig. 3] suggesting, together with the lack of constriction in the hysteresis loop, that magnetization reversal occurs either by coherent or incoherent rotation. This is opposite to the case where the H_{FC} is applied along the major axis of the ellipses. In this case, the MFM images at remanence do not reveal a simple dipolar contrast but a regular arrangement of dark and bright regions [see panel (b.1) in Fig. 3] indicative of the occurrence of a double-vortex state.[15] Correspondingly, the loops exhibit a more pronounced constriction. At sufficiently strong negative magnetic fields, the saturated state is reached and, consequently, dipolar contrast is observed [see panels (a.2) and (b.2)]. For the sake of clarity, the spin configurations and the MFM images simulated using a lift height of 100 nm, corresponding to panels (a.1), (a.2), (b.1), and (b.2), are shown in panels (a.3) and (a.5), (a.4) and (a.6), (b.3) and (b.5), and (b.4) and (b.6), respectively. For larger angles of measurement, the ellipses reverse without forming vortex states (regardless of the thermomagnetic history of the sample).

It is worth mentioning that the transition from magnetization reversal via vortex formation to rotation of incoherent magnetization states with increasing angle between the magnetic field and FC direction was already reported for circular dots. This was ascribed to the competition between magnetostatic and exchange energies.[8] In the ellipses, for FC along the major axis, setting exchange bias along the major axis of the ellipse is analogous to increasing shape anisotropy, which will favor coherent rotation over vortex reversal when measured parallel to the major axis. However, this does not explain why vortex reversal should be observed at intermediate angles. Interestingly, the MFM images in Fig. 3(b) reveal that the constricted loop for FC along the major axis is associated with the formation of not one but two vortices in the ellipse. Previous reports have shown that $Ni_{80}Fe_{20}$ ellipses will reverse via two vortices for fields applied along the major axis and by single vortex when the field is applied along the minor axis.[15] In Fig. 3(b), the measurement angle is closer to the minor axis; however, whenever there is an angle between the exchange bias and the measurement direction, an *S*-state curvature will be introduced into the spin distribution as the field is reduced. This configuration will favor the formation of two vortices of opposing chiralities, a state that is metastable in these ellipses, provided the relative fields are such that nucleation can be established. Interestingly, the chirality of the two-vortex state is the same for the various ellipses that were imaged indicating that a preferred direction for the spins along the ellipse edges is favored by the exchange bias. Thus, the exchange bias can be used to stabilize

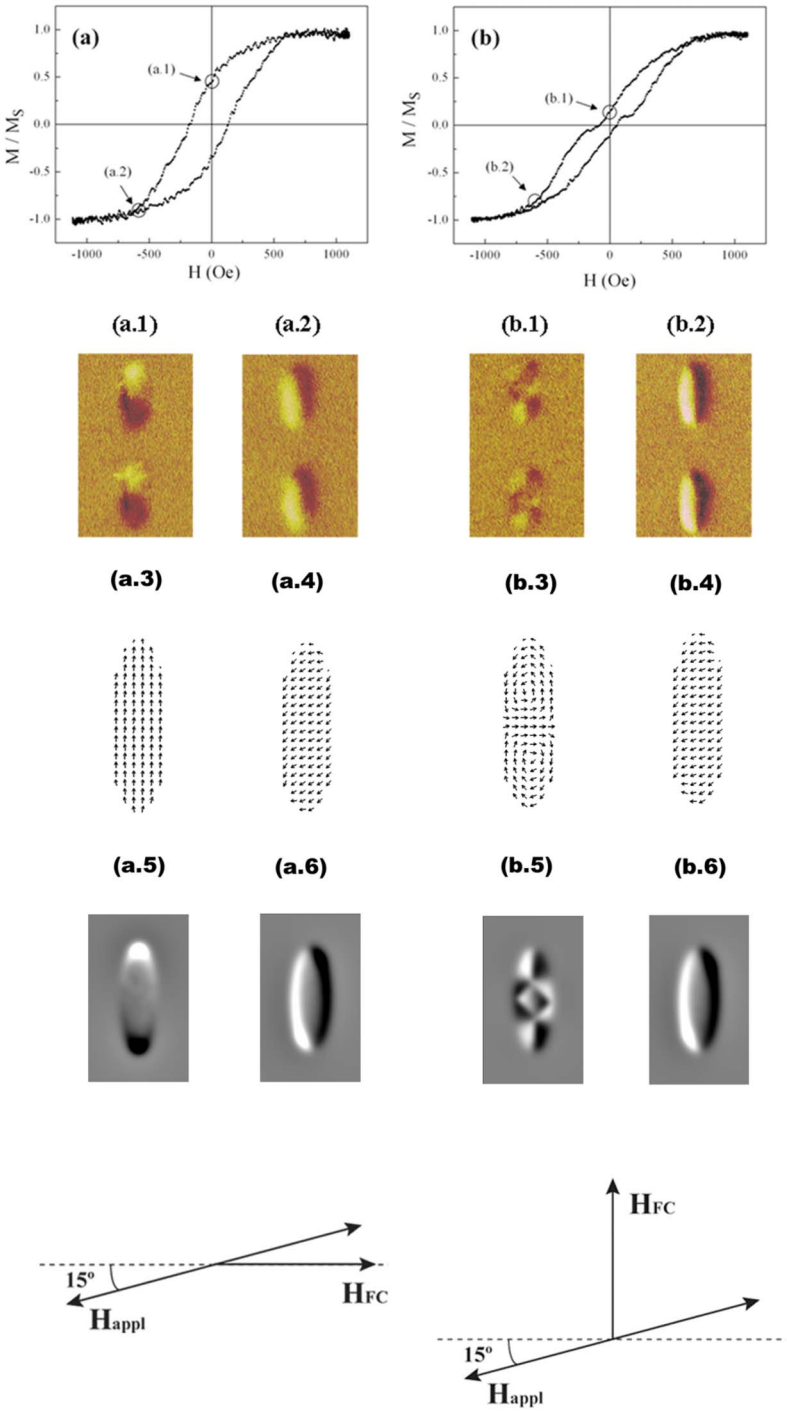

FIG. 3. (Color online) (a) Hysteresis loop corresponding to the $0.5 \times 1.5\ \mu m^2$ $Ni_{80}Fe_{20}/Ir_{20}Mn_{80}$ ellipses measured at 15° from the minor axis after FC along the minor axis of the ellipses. Panels (a.1) and (a.2) are the MFM images obtained at remanence and applying a field of −550 Oe, respectively; panels (a.3), (a.4), (a.5), and (a.6) are the corresponding spin configurations and simulated MFM images. (b) Hysteresis loop of the same ellipses, also measured at 15° from the minor axis, after FC along the major axis of the ellipses. Panels (b.1) and (b.2) are the corresponding MFM images at remanence and with an applied field of −550 Oe, respectively; panels (b.3), (b.4), (b.5), and (b.6) are the corresponding spin configurations and simulated MFM images.

a vortex-pair state with specific chiralities at angles close to the minor axis of the ellipses when exchange bias is induced along their major axis.

CONCLUSIONS

In summary, exchange biased ellipses have been found to reverse by formation of a vortex state when they are FC and measured along their minor axis, while mainly single domain states are observed after FC and measurement along their major axis. For the most elongated ellipses (aspect ratio of 3), the magnetization reversal mechanism of these dots can be tailored to either favor or suppress the formation of a vortex-pair magnetization state through the choice of off-axis measurement angle and the direction of the exchange bias. Hence, our work may open up new perspectives toward the utilization of lithographed elliptical dots in spintronic micron and submicron devices.

ACKNOWLEDGMENTS

Financial support from the 2005SGR-00401, the MAT-2007-66302-C02, and the HF2006-0197 research projects is acknowledged. Work at Argonne, including the use of facilities at the Center for Nanoscale Materials, was supported by the U.S. Department of Energy under Contract No. DE-AC02-06CH11357. E.M. acknowledges his FPI fellowship

from the Spanish Ministerio de Educación y Ciencia, cofinanced by the ESF.

[1]J. Nogués and I. K. Schuller, J. Magn. Magn. Mater. **192**, 203 (1999); M. Kiwi, *ibid.* **234**, 548 (2001); R. L. Stamps, J. Phys. D **33**, R247 (2000); A. E. Berkowitz and K. Takano, J. Magn. Magn. Mater. **200**, 552 (1999).
[2]J. Nogués, J. Sort, V. Langlais, S. Suriñach, V. Skumryev, J. S. Muñoz, and M. D. Baró, Phys. Rep. **422**, 65 (2005).
[3]M. D. Stiles and R. D. McMichael, Phys. Rev. B **63**, 064405 (2001); **60**, 12950 (1999); **59**, 3722 (1999); C. Leighton, M. R. Fitzsimmons, A. Hoffmann, J. Dura, C. F. Majkrzak, M. S. Lund, and I. K. Schuller, *ibid.* **65**, 064403 (2002).
[4]B. Dieny, V. S. Speriosu, S. S. P. Parkin, B. A. Gurney, D. R. Wilhoit, and D. Mauri, Phys. Rev. B **43**, 1297 (1991).
[5]J. Sort, S. Suriñach, J. S. Muñoz, M. D. Baró, J. Nogués, G. Chouteau, V. Skumryev, and G. C. Hadjipanayis, Phys. Rev. B **65**, 174420 (2002); J. Sort, J. Nogués, X. Amils, S. Suriñach, J. S. Muñoz, and M. D. Baró, Appl. Phys. Lett. **75**, 3177 (1999); L. Bessais, S. Sab, C. Djéga-Mariadassou, N. H. Dan, and N. X. Phuc, Phys. Rev. B **70**, 134401 (2004).
[6]J. Nogués, V. Skumryev, J. Sort, S. Stoyanov, and D. Givord, Phys. Rev. Lett. **97**, 157203 (2006); V. Skumryev, S. Stoyanov, Y. Zhang, G. Hadjipanayis, D. Givord, and J. Nogués, Nature (London) **423**, 850 (2003).
[7]M. Fraune, U. Rüdiger, G. Güntherodt, S. Cardoso, and P. Freitas, Appl. Phys. Lett. **77**, 3815 (2000); E. Girgis, R. D. Portugal, H. Loosvelt, M. J. Van Bael, I. Gordon, M. Malfait, K. Temst, and C. Van Haesendonck, Phys. Rev. Lett. **91**, 187202 (2003); V. Baltz, J. Sort, S. Landis, B. Rodmacq, and B. Dieny, *ibid.* **94**, 117201 (2005); S. H. Chung, A. Hoffmann, and M. Grimsditch, Phys. Rev. B **71**, 214430 (2005); A. Hoffmann, M. Grimsditch, J. E. Pearson, J. Nogués, W. A. A. Macedo, and I. K. Schuller, *ibid.* **67**, 220406 (2003).
[8]J. Sort, A. Hoffmann, S. H. Chung, K. Buchanan, M. Grimsditch, M. D. Baró, B. Dieny, and J. Nogués, Phys. Rev. Lett. **95**, 067201 (2005).
[9]J. Sort, K. S. Buchanan, V. Novosad, A. Hoffmann, G. Salazar-Alvarez, M. D. Baró, B. Dieny, and J. Nogués, Phys. Rev. Lett. **97**, 067201 (2006); J. Sort, G. Salazar-Alvarez, M. D. Baró, B. Dieny, A. Hoffmann, V. Novosad, and J. Nogués, Appl. Phys. Lett. **88**, 042502 (2006).
[10]Z. P. Li, A. Petracic, J. Eisenmenger, and I. K. Schuller, Appl. Phys. Lett. **86**, 072501 (2005); J. Eisenmenger, Z. P. Li, W. A. A. Macedo, and I. K. Schuller, Phys. Rev. Lett. **94**, 057203 (2005); L. J. Chang, A. L. Chen, K. W. Cheng, C. Yu, S. F. Lee, Y. Liou, and Y. D. Yao, J. Appl. Phys. **101**, 09F511 (2007); W. Jung, F. J. Castaño, and C. A. Ross, Phys. Rev. Lett. **97**, 247209 (2006); W. Jung, F. J. Castaño, D. Morecroft, C. A. Ross, R. Menon, and H. I. Smith, J. Appl. Phys. **97**, 10K113 (2005); J. Mejía-López, P. Soto, and D. Altbir, Phys. Rev. B **71**, 104422 (2005).
[11]K. Yu. Guslienko and A. Hoffmann, Phys. Rev. Lett. **97**, 107203 (2006); J. Appl. Phys. **101**, 093901 (2007).
[12]J. C. Wu, H. W. Huang, C. H. Lai, and T. H. Wu, J. Appl. Phys. **87**, 4948 (2000).
[13]D. Paccard, C. Schlenker, O. Massenet, R. Montmory, and A. Yelon, Phys. Status Solidi **16**, 301 (1966); A. Hoffmann, Phys. Rev. Lett. **93**, 097203 (2004); C. Binek, S. Polisetty, X. He, and A. Berger, *ibid.* **96**, 067201 (2006); S. Brems, K. Temst, and C. Van Haesendonck, *ibid.* **99**, 067201 (2007).
[14]M. R. Scheinfein, LLG Micromagnetics Simulator™.
[15]P. Vavassori, N. Zaluzec, V. Metlushko, V. Novosad, B. Ilic, and M. Grimsditch, Phys. Rev. B **69**, 214404 (2004); X. Liu, J. N. Chapman, S. McVitie, and C. D. W. Wilkinson, Appl. Phys. Lett. **84**, 4406 (2004); X. Liu, J. N. Chapman, S. McVitie, and C. D. W. Wilkinson, J. Appl. Phys. **96**, 5173 (2004); I. L. Prejbeanu, M. Natali, L. D. Buda, U. Ebels, A. Lebib, Y. Chen, and K. Ounadjela, *ibid.* **91**, 7343 (2002).
[16]Y. C. Chang, C. C. Chang, and J. C. Wu, IEEE Trans. Magn. **41**, 3742 (2005).
[17]J. Yu, A. D. Kent, and S. S. P. Parkin, J. Appl. Phys. **87**, 5049 (2000); T. Eimüller, T. Kato, T. Mizuno, S. Tsunashima, C. Quitmann, T. Ramsvik, S. Iwata, and G. Schütz, Appl. Phys. Lett. **85**, 2310 (2004).